Primary pulmonary intravascular large B-cell lymphoma: Indications from cytomorphology findings through CT-guided puncture: A case report

WEI JIANG[1*], MANGUI LI[2*], CHI ZHANG[3] and XUE XING[1]

[1]Department of Clinical Laboratory, The Second Hospital of Dalian Medical University, Dalian, Liaoning 116000, P.R. China; [2]Department of Clinical Laboratory, Qinghai Red Cross Hospital Laboratory, Xining, Qinghai 810000, P.R. China; [3]Department of Laboratory Medicine, Tongji Hospital, Tongji Medical College, Huazhong University of Science and Technology, Wuhan, Hubei 430030, P.R. China

Received June 20, 2024; Accepted October 4, 2024

DOI: 10.3892/ol.2024.14792

Abstract. Primary pulmonary intravascular large B-cell lymphoma (IVLBCL) is a rare malignant extranodal lymphoma, and it presents symptoms similar to those of lung diseases. Diagnosis of IVLBCL can be challenging and often requires histopathological examination of affected tissues. The present report describes a 65-year-old female patient presenting with a fever, without generalized lymph node enlargement. A CT scan revealed subpleural ground-glass opacities in the upper lobe of the right lung. The lactate dehydrogenase, erythrocyte sedimentation rate and CRP levels were all elevated. The patient had been misdiagnosed with pneumonia by multiple hospitals, and treatments with anti-infective and anti-inflammatory therapies proved ineffective. Subsequently, the patient underwent a CT-guided puncture biopsy of the lesion in the upper lobe of the right lung at the Second Hospital of Dalian Medical University (Dalian, China). Based on the cell morphology, combined with clinical manifestations and other laboratory tests, the possibility of lymphoma was considered. The diagnosis was subsequently confirmed by histopathological examination. To the best of our knowledge, this is the first description of the features of IVLBCL cells under a microscope using an oil-immersion objective lens.

Correspondence to: Dr Xue Xing, Department of Clinical Laboratory, The Second Hospital of Dalian Medical University, 467 Zhongshan Road, Dalian, Liaoning 116000, P.R. China
E-mail: dyeyxx39198645@126.com

Dr Chi Zhang, Department of Laboratory Medicine, Tongji Hospital, Tongji Medical College, Huazhong University of Science and Technology, 1095 Jiefang Avenue, Wuhan, Hubei 430030, P.R. China
E-mail: zccdfile@163.com

*Contributed equally

Key words: pulmonary B-cell lymphoma, intravascular lymphoma, cytomorphology, ground-glass opacity, CT-guided puncture cytology

Introduction

Intravascular large B-cell lymphoma (IVLBCL) is a rare extranodal lymphoma characterized by the proliferation of lymphoma cells almost within the lumina of large and small vessels (1,2). Its pathogenesis remains obscure but is likely related to changes in cell migration properties and endothelium adhesion molecules inhibiting the extravasation of lymphocytes (3). IVLBCL has an estimated incidence rate of ~0.5 cases per million individuals worldwide (4). Due to its unique presentation, the diagnosis of IVLBCL is often delayed, as its clinical symptoms can vary widely and affect multiple organ systems, including the skin, central nervous system and bone marrow (5). Consequently, patients may present with a range of nonspecific symptoms such as fever, respiratory distress and ground-glass opacities (GGOs) (1). The R-CHOP regimen, which includes rituximab, cyclophosphamide, doxorubicin, vincristine and prednisone, is commonly used for treatment (1). Early recognition and diagnosis are crucial for improving prognosis. Previous data show that the median survival time of patients with IVLBCL is ~1 year, and the prognosis is poor (5). Staging of IVLBCL is difficult and still not satisfactory (1). Therefore, differentiating IVLBCL from pneumonia and interstitial lung disease presents a diagnostic challenge (6).

In the present case, a CT-guided biopsy of the lesion was performed. While the pathological morphology has been previously reported (1,7), the cytological morphological characteristics of IVLBCL cells under a microscope with an oil-immersion objective lens were described in the present report. The present case report offers valuable insights that may serve as a crucial reference for improving early clinical identification and diagnosis of IVLBCL.

Case report

A 65-year-old female patient presented to The Second Hospital of Dalian Medical University (Dalian, China) in October 2023, and experienced persistent cough and expectoration lasting for 4 months, accompanied by intermittent fever with fluctuating temperatures of ~37.3˚C. Chest CT scans performed

at Wafangdian Central Hospital (Dalian, China) and Dalian Central Hospital (Dalian, China) revealed scattered subpleural GGO in both lungs, prompting suspicion of bacterial, viral or other pathogenic infections. Treatment with levofloxacin, penicillin (dosage unspecified) and oral prednisone (reducing dose from 50 to 15 mg) yielded no significant improvement. At 5 days before admission to the respiratory department (The Second Hospital of Dalian Medical University, Dalian, China) in October 2023, the temperature of the patient reached 38.2˚C. A subsequent chest CT scan revealed multiple round GGOs in the subpleural regions of both lungs, suggesting viral pneumonia (Fig. 1A and B).

Upon admission, the detection of extractable nuclear antigen (ENA) was performed using a Diagnostic Kit for ENA (cat. no. ENA-17; Guangzhou Kangrun Biotech Co., Ltd.) on a fully automated immunoblot analyzer (HELIA BLOT; Guangzhou Kangrun Biotech Co., Ltd.) using the immunoblotting method, and this was negative, indicating that the patient did not have an autoimmune disease. The results of tumor markers, including α-fetoprotein, carbohydrate antigen (CA)-199, CA-242, CA-125, CA-153, carcinoembryonic antigen (CEA), prostate-specific antigen and neuron-specific enolase (NSE), detected using an electrochemiluminescence method (Shenzhen New Industries Biomedical Engineering Co., Ltd.), were all within the normal range. Bronchoscopy and bronchoalveolar lavage detected no abnormal cells. However, hemoglobin and albumin levels were decreased, while serum ferritin, lactate dehydrogenase and inflammatory marker levels were elevated compared with the normal range (Table I), indicating a possible tumor. The clinicians performed a CT-guided puncture biopsy of the lesion in the upper lobe of the right lung. The procedure was conducted smoothly. At the conclusion of the lung puncture, upon removal of the puncture needle, a synchronous CT scan revealed a small amount of needle-induced bleeding at the puncture site. No gas shadows were observed in the heart or major vessels, and no other complications were noted (Fig. 1C). The smear was then sent to the laboratory for cytological examination. After 20 min of Wright-Giemsa staining [Wright's stain: 1 g of dried Wright's stain was placed in a mortar and 500 ml methanol (concentration, ≥99.8%) was added, followed by grinding at room temperature until the stain was dissolved. Giemsa Stain: 7.6 g Giemsa stain powder was dissolved in 500 ml methanol and 500 ml glycerol wad added, followed by grinding at room temperature until the stain was dissolved. Solution A: Wright's stain and Giemsa's stain were mixed at a ratio of 10:1 for use. Solution B: Buffer solution (pH 6.4-6.8; weakly acidic): 30 ml 1% KH_2PO_4, 20 ml 1% Na_2HPO_4 and H_2O (fresh) up to 1,000 ml. Staining was performed at room temperature. First, at room temperature, 0.5 ml of Solution A (Solution A contains a fixative with a concentration of methanol ≥99.8%) was added for fixation for 30 sec, and then 1 ml Solution B was added for staining for 18 min, followed by rinsing with tap water and drying for 2 min], observation under an Olympus BX43 (Olympus Corporation) light microscope using an oil-immersion objective lens revealed clusters of abnormal cells. These cells were slightly larger than mature lymphocytes, round or oval in shape; with large nuclei, smooth in outline, oval to irregular, uniform and delicate chromatin; with indistinct or occasional nucleoli; with scant cytoplasm, some with vacuoles; and exhibited an embedded and adhesion-like pattern (Fig. 2). Considering the size, arrangement and morphological features of the abnormal cells, along with the prevalence of various lung malignancies, small cell lung cancer (SCLC) was initially suspected (8). However, SCLC typically presents as a hilar mass and bulky mediastinal lymphadenopathy that cause persistent cough and dyspnea. Furthermore, SCLC is characterized by a rapid doubling time, high growth fraction and early development of widespread metastases (9). In the present case, the presentation of the patient diverged markedly from these hallmarks of SCLC, and tumor markers such as NSE, CEA and CA-125 were negative. Given these discrepancies, it was possible to provisionally exclude the diagnosis of SCLC. For the malignant tumor cells with this morphological appearance, the initial suspicion was lymphoma cells. The morphology and arrangement of the cells were not consistent with diffuse large B-cell lymphoma (DLBCL) (10), and the mediastinum and other lymph nodes were not enlarged, and thus, DLBCL cells were also excluded. The cellular morphology observed by oil immersion microscopy differed from that reported for small cell carcinoma and DLBCL (8,10). Combined with the aforementioned clinical presentation and examination results, this raised the suspicion of primary pulmonary intravascular lymphoma (8-10). Therefore, it was strongly recommended that the patient should be transferred to the hematology department, and that pathology and immunohistochemical staining should be performed. H&E staining revealed capillary or sinusoidal structures. The tissues were fixed in 10% neutral formalin overnight at room temperature for 12 h. The slices (thickness, 4 μm) were placed in xylene I for 10 min, xylene II for 10 min, anhydrous ethanol I for 1 min, anhydrous ethanol II for 1 min, 95% ethanol I for 1 min, 95% ethanol II for 1 min, 90% ethanol for 1 min and 80% ethanol for 1 min, and then washed with tap water for 1 min. The sections were then stained with Harris hematoxylin for 1 min at room temperature, washed with tap water for 1 min, differentiated with 1% hydrochloric acid ethanol for 30 sec at room temperature, and rinsed with tap water for 5 min. The sections were then stained in eosin staining solution at 37˚C for 30 sec, and washed with tap water for 30 sec. Thereafter, the slices were placed into 85% ethanol for 20 sec, 90% ethanol for 30 sec, 95% ethanol I for 1 min, 95% ethanol II for 1 min, absolute ethanol I for 2 min, absolute ethanol II for 2 min, and xylene I, xylene II and xylene III for 2 min, respectively. After the last step, the slices were removed from xylene and dried before being sealed with neutral gum. Finally, the slides were examined under a light microscope (Olympus Corporation) and images were acquired. Within these small blood vessels, individual or small clusters of tumor cells were observed. The cells exhibited consistent morphology with marked atypia, large deeply stained nuclei, and no transitional zone between the tumor cells and the surrounding lung tissue (Fig. 3A). Based on the morphological characteristics, the pathologist initially suspected lymphoma (1). Subsequently, immunohistochemistry (IHC) was performed. ICH detection kits, which included ready-to-use blocking reagents, primary and secondary antibodies, and other necessary reagents that required no dilution, were used according to the instructions provided with each kit. The antibody kits used included AE1/AE3 (cat. no. ZM-0069), CD20 (cat. no. ZM-0039), CD5 (cat. no. ZA-0510), CD10 (cat. no. ZM-0283), Bcl-6

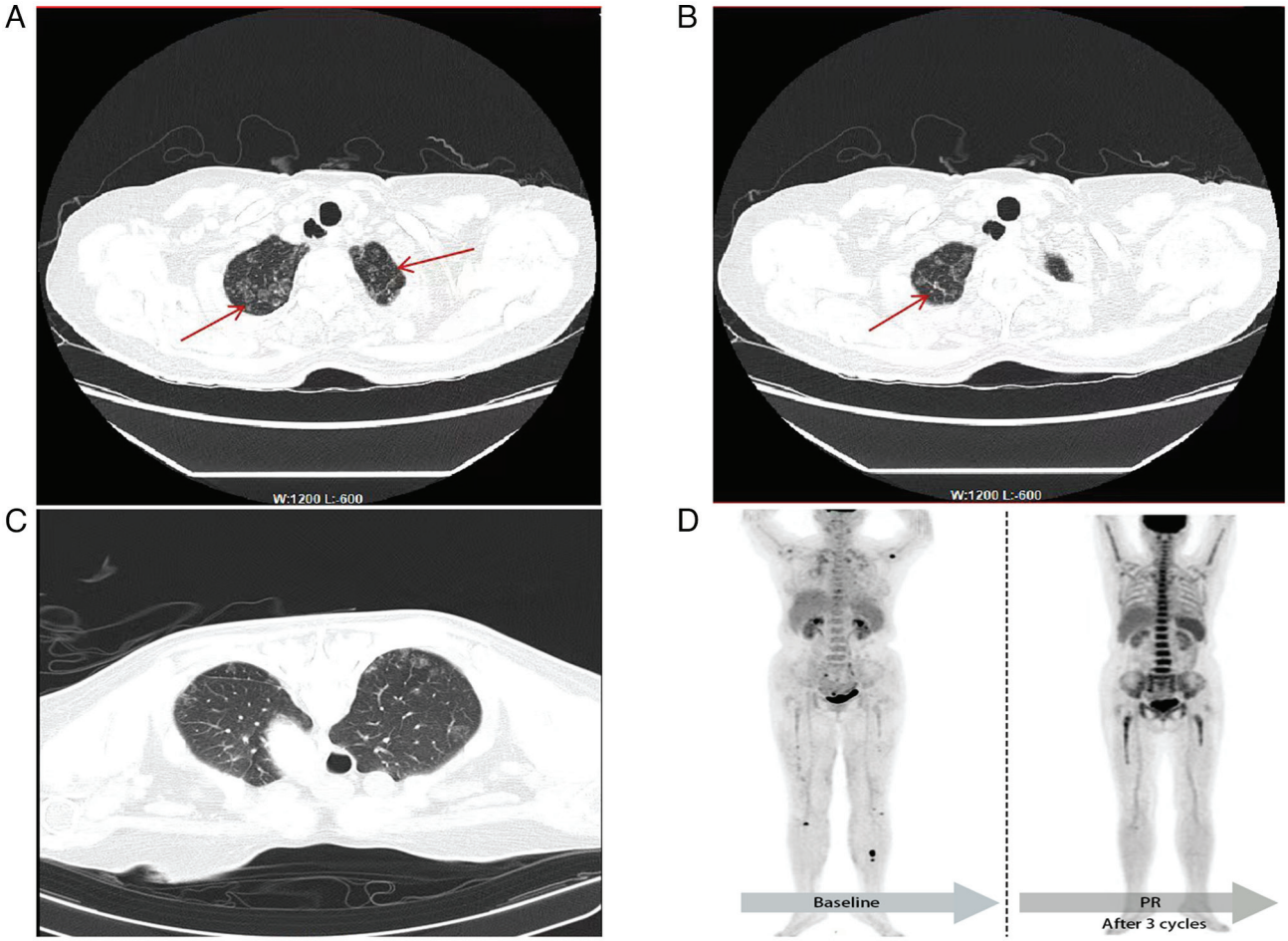

Figure 1. (A) Multiple roundish GGO in both upper lungs (arrows). (B) Thickening of the interlobular septa (arrow), and GGO were present in admixture with thickening of the interlobular septa. (C) Image showing that no pneumothorax and other complications occurred after the puncture. (D) Baseline image showing intensive fluorodeoxyglucose uptake in multiple sites throughout the body. Follow-up image after 3 cycles of the combination chemotherapy showing a PR. GGO, ground-glass opacities; PR, partial response.

(cat. no. ZM-0011), Bcl-2 (cat. no. ZA-0536), multiple myeloma oncogene 1 (MUM1; cat. no. ZA-0583), C-Myc (cat. no. ZA-0555), CyclinD1 (cat. no. ZM-0039), p53 (cat. no. ZM-0408), CD34 (cat. no. ZM-0046), CD30 (cat. no. ZM-0043) and Ki-67 (cat. no. ZM-0166), all of which were purchased from Beijing Zhongshan Jinqiao Biotechnology Co., Ltd. The tissues were fixed in 10% neutral formalin overnight at room temperature for 12 h. After sectioning the samples to a thickness of 4 μm, deparaffinization and hydration (at room temperature by soaking in anhydrous ethanol, 95% ethanol and 85% ethanol for 3 min each, followed by a 1-min rinse with tap water) pretreatments were conducted. The EDTA antigen retrieval solution was heated to boiling in a stainless steel pot on an induction cooker at high power, and then the sections were placed on a heat-resistant slide rack and immersed in the retrieval solution to heat for 20 min. Subsequently, the solution was allowed to cool naturally for 10 min, and once the liquid in the pot had cooled to room temperature, the sections were removed and rinsed with distilled water for 3 min twice. A drop of endogenous peroxidase blocking agent was added and sections were incubated at room temperature for 10 min. Subsequently, 100 μl primary antibody was added and sections were incubated at room temperature for 60 min, followed by the addition of 100 μl enzyme-labeled secondary antibody and incubation for an additional 15 min at room temperature. For chromogenic staining, 3,3'-diaminobenzidine (DAB) was used, and sections were incubated at room temperature for 3-5 min, rinsed with tap water and counterstained with hematoxylin for 5 min at room temperature. Finally, the location and intensity of the markers were observed under a light microscope. Additionally, *in situ* hybridization Epstein-Barr encoding region (EBER) detection was performed. The EBER detection kit (cat. no. ISH-7001; Beijing Zhongshan Jinqiao Biotechnology Co., Ltd.), which included blocking reagent, pepsin and HRP-conjugated anti-digoxigenin antibody (all reagents were ready to use without dilution), was used according to the manufacturer's instructions. The tissues were fixed in 10% neutral formalin overnight at room temperature for 12 h. After fixation, the tissue was paraffin-embedded. After sectioning the samples to a thickness of 4 μm, the sections were placed in deparaffinization solution and soaked for 10 min, which was repeated three times. After removing the excess liquid, the sections were placed in anhydrous ethanol for soaking for 3 min, which was repeated three times. The sections were then air-dried for 10 min. Subsequently, 100 μl blocking solution was added, and the sections were incubated at room temperature in the dark for 10 min. After washing off the blocking solution with pure water, gradient ethanol dehydration was performed at room

Table I. Laboratory findings of the patient.

Variable, unit (RI)	Pre-ADM	Pre-ADM	ADM	Post-ADM	Post-ADM	Post-ADM
Hospitalization day	-98	-17	0	23	44	65
Treatment phase	-	-	Baseline R-CHOP	Post-C1 R-CHOP	Post-C2 R-CHOP	Post-C3 R-CHOP
HB, g/l (115-150 g/l)	91	88	77	94	102	111
Alb, g/l (40-55 g/l)	24.00	22.74	23.90	32.58	34.54	37.21
ESR, mm/h (0-20 mm/h)	80	106	105	67	19	20
CRP, mg/l (0-10 mg/l)	36.28	44.93	100.07	11.00	3.33	3.64
FER, ng/ml (10-291 ng/ml)	399.41	726.76	721.64	76.85	-	-
PCT, ng/ml (0-0.06 ng/ml)	0.02	0.16	0.09	-	-	-
LDH, U/l (120-250 U/l)	-	281.25	329.81	286.72	189.58	253.60
IL-2R, U/ml (223-710 U/ml)	236	-	4382	671	562	669
IL-6, pg/ml (0-3.4 pg/ml)	17.9	-	49.0	5.9	7.1	4.5
IL-10, pg/ml (0-9.1 pg/ml)	126.8	-	>1,000.0	<5.0	<5.0	5.8
TNF-α, pg/ml (0-8.1 pg/ml)	1.4	-	13.9	10.6	16.1	20.5

ADM, admission; HB, hemoglobin; Alb, albumin; ESR, erythrocyte sedimentation rate; FER, ferritin; PCT, procalcitonin; LDH, lactate dehydrogenase; IL-2R, interleukin-2 receptor; Post-C, post-cycle; R-CHOP, rituximab, cyclophosphamide, doxorubicin, vincristine and prednisone; RI, reference interval; -, not measured.

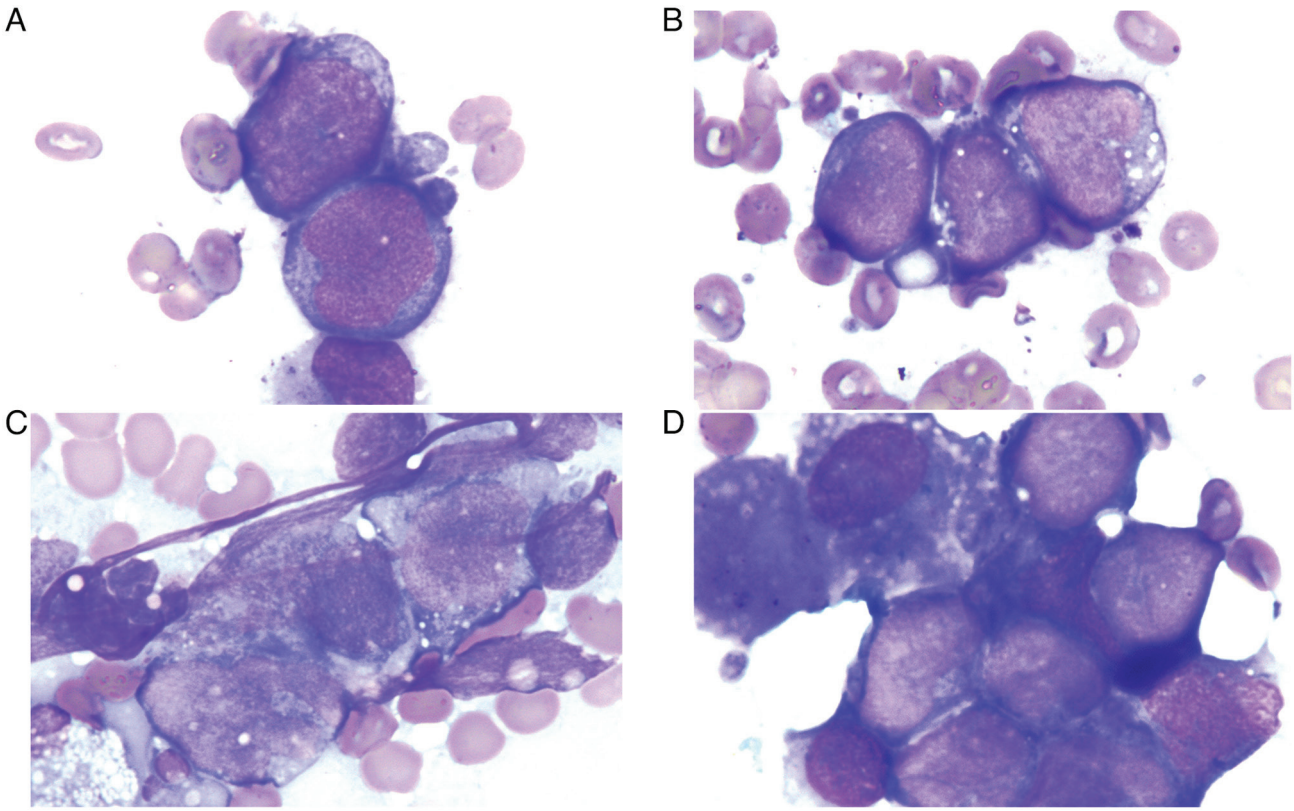

Figure 2. (A) Lung primary IVLBCL cells were round or oval in shape, with large nuclei, and smooth in outline. (B) IVLBCL cells had scant cytoplasm, some with vacuoles, and exhibited an embedded and adhesion-like pattern. (C) IVLBCL cells were oval to irregular, with uniform and delicate chromatin, and had indistinct or occasional nucleoli. (D) IVLBCL cells exhibited an embedded and adhesion-like pattern. (A-D) All stained with Wright-Giemsa stain; magnification, x1,000. IVLBCL, intravascular large B-cell lymphoma.

temperature (75, 95 and 100% for 2 min each), followed by air-drying. Subsequently, 100 μl pepsin solution was added, and the sections were incubated at 37˚C for 20 min. After discarding the pepsin solution, gradient ethanol dehydration was carried out at room temperature (75, 95 and 100% for 2 min each), followed by air-drying. Next, 10 μl digoxigenin-labeled EBER

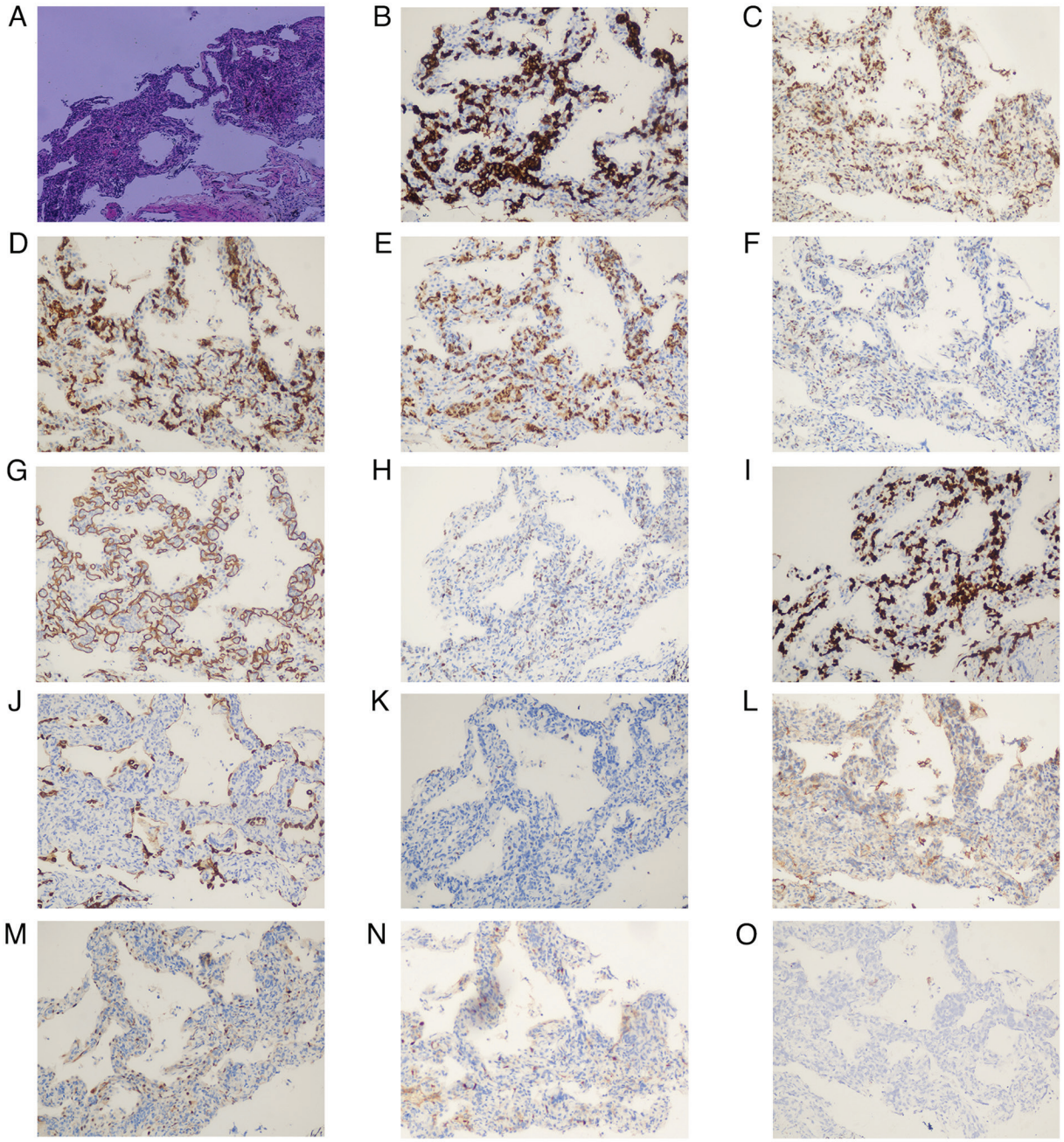

Figure 3. (A) Lung tissue specimens stained with H&E stain. Within the small blood vessels, individual or small clusters of tumor cells were observed (magnification, x100). (B) CD20 positive. (C) Bcl-6 positive. (D) Bcl-2 diffuse strong positive. (E) Multiple myeloma oncogene 1 positive. (F) p53 positive (30%+). (G) CD34 positive (vessels+). (H) C-Myc positive (30%+). (I) Ki-67 positive (>90%). (J) AE1/AE3 negative. (K) CD5 negative. (L) CD10 negative. (M) CyclinD1 negative. (N) CD30 negative. (O) Epstein-Barr encoding region negative. (B-O) All magnification, x200.

probe was added, and the sections were covered with a silanized cover slip, and sealed with rubber cement. The sections were hybridized and incubated at 37˚C for 4 h (*in situ* hybridization was performed in a moist chamber). The rubber cement was carefully removed, and the slides were immersed in PBS buffer for 10 min, allowing the cover slips to fall off naturally. A hydrophobic pen was used to draw a circle around the tissue. The slides were then rinsed with PBS buffer for 2 min, which was repeated three times. All aforementioned operations were carried out at room temperature. Subsequently, 50 μl HRP-conjugated anti-digoxigenin antibody was added, and the sections were incubated at 37˚C for 30 min, followed by rinsing with PBS buffer for 2 min, which was repeated three times. Freshly prepared DAB chromogenic solution was added at room temperature, and the sections were incubated for 10 min. The sections were then rinsed with tap water, counterstained with hematoxylin at room temperature for 10 sec, differentiated and rinsed to blue. Finally, the sections were dehydrated and cleared, and the result was observed under a light microscope. The IHC and EBER results were issued by the pathology department 2 days later. The results showed AE1/AE3 (-) (Fig. 3J), which primarily ruled out an epithelial origin of the tumor (11), and CD20 (+) (Fig. 3B), CD5 (-) (Fig. 3K), CD10 (-) (Fig. 3L), Bcl-6 (+) (Fig. 3C), Bcl-2 (diffuse strong+) (Fig. 3D), MUM1 (+) (Fig. 3E), C-Myc (30%+) (Fig. 3H), CyclinD1 (-) (Fig. 3M), p53 (30%+) (Fig. 3F), CD34 (vessels+) (Fig. 3G),

CD30 (-) (Fig. 3N), Ki-67 (+; >90%) (Fig. 3I) and EBER (-) (Fig. 3O). The patient was ultimately diagnosed with IVLBCL (2). In the present case, the patient declined molecular biological and genetic testing. Subsequent positron emission tomography-CT (PET-CT) demonstrated metabolic enhancement in multiple sites throughout the body (Fig. 1D), involving the lung, bone, bone marrow, pituitary gland, right temporal region and various subcutaneous soft tissues, and the clinical stage was IV (1,12). Treatment with rituximab (600 mg), cyclophosphamide (1.3 g), doxorubicin (80 mg), vincristine (2 mg) and prednisone (15 mg) (R-CHOP) combined with zanubrutinib (160 mg) was administered for 7 cycles over a total of 150 days, causing the hemoglobin levels to gradually increase, while the erythrocyte sedimentation rate, CRP, ferritin, lactate dehydrogenase, and inflammatory cytokine levels gradually decreased to normal levels and a stable clinical condition (Table I). Currently, the interim PET-CT revealed a reduction in the extent of GGO and a decrease or complete resolution of abnormal glucose metabolism throughout the body (Fig. 1D). The patient was advised to have follow-up appointments every 3 months, which would likely include blood tests, imaging studies and physical examinations to monitor for any signs of recurrence or complications. The patient was in good condition in July 2024.

Discussion

Clinically, IVLBCL predominantly affects the elderly, with no significant sex disparity in prevalence (5). Currently, IVLBCL is clinically categorized into three variants based on presentation: Cutaneous, classic and hemophagocytic. These variants exhibit varying prognoses, with the cutaneous variant generally being associated with an improved outcome in young women in Western countries (1). The hemophagocytic variant is more prevalent in Asian countries, accounting for 79% of IVLBCL cases in Asia (13), and is characterized by multiorgan failure, hepatosplenomegaly and pancytopenia. The present case, exhibiting primary lung involvement and persistent anemia without leukopenia or thrombocytopenia, was a classic variant with pulmonary primary IVLBCL and a rare manifestation in Asian patients.

Similar to the present case, a number of patients with primary pulmonary IVLBCL have been easily misdiagnosed with pneumonia or even overlooked, treated with steroids and experienced worsening symptoms (14,15). The diagnosis frequently took over a month or longer from atypical symptom onset (16), and some patients were diagnosed incidentally (17). Yamamoto *et al* (18) reported a case of IVLBCL in which the patient showed no overt symptoms but was incidentally found to have multiple GGOs during examination for a pancreatic cyst. A subsequent surgical lung biopsy led to the diagnosis of IVLBCL. In this instance, pulmonary IVLBCL may have progressed slowly without noticeable symptoms (18). IVLBCL is likely to be overlooked because it does not form visible extravascular masses, and only autopsy can confirm it (19). An autopsy review revealed pulmonary involvement in ~60% of cases (20), while a single-center study found diffuse GGO on chest CT in 23.8% of patients (21). Therefore, early diagnosis of primary pulmonary IVLBCL remains a clinical challenge.

Screening methods for primary pulmonary IVLBCL mainly include random skin biopsy, PET-CT, bronchoscopy brushings, bronchoalveolar lavage, transbronchial lung biopsy (TBLB) and surgical tissue biopsy (15,16,21-28). Studies have indicated that most IVLBCL lesions exist within the subcutaneous adipose tissue vessels, and random skin biopsy can be used for early diagnosis (21-23). However, this method has limitations, with lower sensitivity and potential false-negative results due to the variations in skin biopsy puncture depth and location (24). Due to the high incidence of cutaneous melanoma in Western countries, the diagnostic efficiency of random skin biopsy is relatively high in Western countries (25). PET-CT is used in the early diagnosis of isolated pulmonary IVLBCL (26,27). However, Zhu *et al* (15) found that only 1 case in their study presented pulmonary mild ^{18}F-fluorodeoxyglucose (FDG) uptake on PET, which was atypical. Furthermore, Nguyen *et al* (16) reported that 3 patients (including 1 of the autopsied patients) failed to demonstrate any parenchymal FDG uptake in the lungs. GGO imaging findings in the lungs are nonspecific for this disease, and bronchoscopy brushings or bronchoalveolar lavage have limited sampling sites and specimen volumes (28). TBLB may occasionally yield the evidence of lung involvement with IVLBCL; however, the small size of the bronchoscopic biopsy specimens limits its sensitivity in diagnosing microvascular disease processes such as IVLBCL (16). Compared with surgical tissue biopsy, CT-guided percutaneous biopsy is a precise and minimally invasive method. Furthermore, additional insights can be provided by quickly staining the punctured cells under a microscope.

To the best of our knowledge, the present report was the first to provide a morphological description of primary pulmonary IVLBCL cells under an oil-immersion objective. The size and arrangement of IVLBCL cells resembled those of SCLC. Based on the observations in the present case, IVLBCL cells exhibited chromatin (uniform and delicate, with visible nucleoli and less cytoplasm) that is more similar to that of original immature lymphocytes. However, SCLC cells (8) are more regular in shape, round, ovate or angular, with finely granular or deeply stained chromatin, and no or inconspicuous nucleoli, and have sparse cytoplasm compared with IVLBCL cells. Furthermore, IVLBCL cells need to be distinguished from lung-infiltrating DLBCL cells (10), which are larger, have more pronounced nucleoli, more cytoplasm and a diffusely distributed pattern; however, IVLBCL cells exhibit an embedded and adhesion-like pattern. Therefore, the aforementioned three types of cells can be identified based on morphology and distribution pattern. Additionally, both Hodgkin's lymphoma (HL) and infectious mononucleosis (IM) initially present with fever in the early clinical stage (29,30). However, the morphological characteristics of HL include typical Reed-Sternberg cells (29), while IM is characterized by the presence of typical atypical lymphocytes (30), both of which can be distinguished from IVLBCL. Combined with clinical manifestations (such as enlarged lymph nodes and laboratory tests), morphology can provide important clues for the diagnosis of IVLBCL.

Studies on the molecular biology and cytogenetics of IVLBCL are scarce. Only a limited number of investigations have reported on the clonal rearrangement, gene mutations and chromosomal rearrangements of the immunoglobulin heavy chain in this rare disease (15,31-34). Tanaka *et al* (31) found that lymphoplasmacytic lymphoma clones utilize the J4 segment of

the immunoglobulin heavy chain gene, while IVLBCL clones utilize the J6 segment. Next-generation sequencing analysis has indicated that IVLBCL exhibits a non-germinal center B-cell gene expression profile, characterized by hyperactivation of the NF-κB pathway (32). Furthermore, high mutation frequencies have been observed in several genes, including MYD88 (57%), CD79B (67%), SETD1B (57%) and major histocompatibility complex, class I, B (57%) (33). Fujikura *et al* (34) found that most cases of their archive had recurrent abnormalities in chromosomes 6, 8 and 19, with the most common being 6q13, 8p11 and 19q13, and chromosome 4/8 losses and marker chromosomes were also detected in the study. In a case report of primary pulmonary IVLBCL, Zhu *et al* (15) detected gene recombination of Igκ-VJ and Igκ-V/in by PCR. In the present case, the patient declined molecular biological and genetic testing. Due to the rarity of primary pulmonary IVLBCL, genetic research specific to this subtype is still lacking.

At present, there is no specific clinical staging standard for IVLBCL. In clinical practice, the Ann Arbor staging system for lymphoma is typically used for assessment (12). The cutaneous variant, involving only a single extranodal organ (skin), is usually classified as stage I (1,12). Notably, patient survival is strongly associated with the number of cutaneous lesions, and although classified as stage I, most patients with multiple skin manifestations suffered a relapse within 1 year of treatment and showed a worse outcome (35). The classic variant and the hemophagocytic variant are characterized by high aggressiveness and rapid disease progression, and they often present with diffuse or widespread extranodal organ involvement at diagnosis, such as the nervous system, bone marrow, spleen and liver, and are therefore typically classified as stage IV (1). IVLBCL is characterized by insidious onset and easy metastasis, and the Ann Arbor staging system (12) is inadequate for accurate assessment, highlighting the need for more precise staging criteria (1).

Current data involve only individual case reports because of the rarity of IVLBCL and lack of prospective multicenter trials providing definitive treatment strategies (4,5,7,14,15,21,24,31). The chemotherapy regimen remains uncertain, and the R-CHOP chemoimmunotherapy remains a first-line option (1,2). The cutaneous variant of IVLBCL, albeit being less aggressive, should be treated in the same way as the other variants (1). Notably, in patients without central nervous system (CNS) involvement at initial diagnosis, the risk of CNS recurrence is as high as 18% in R-CHOP-treated patients (36). Consequently, the addition of drugs with an improved CNS bioavailability, such as high-dose methotrexate, represents a possible strategy (36). Furthermore, capitalizing on the high frequency of MYD88 and CD79 mutations observed in patients with IVLBCL, a clinical trial demonstrated that zanubrutinib plus R-CHOP had promising efficacy and safety as a front-line regimen in IVLBCL, even in patients with CNS involvement (37). Additionally, Kato *et al* (38) suggested that consolidation therapy with autologous stem cell transplantation following remission can serve as an effective treatment strategy.

In the present case, the patient declined genetic testing; however, the clinical symptoms were relieved after R-CHOP treatment. Interim PET-CT revealed a reduction in the extent of GGO and a decrease or complete resolution of abnormal glucose metabolism throughout the body. In the future, close follow-up will be maintained to monitor the long-term prognosis of the patient.

In conclusion, the diagnosis of primary pulmonary IVLBCL is often challenging because of nonspecific signs and symptoms, causing potential misdiagnosis and overlook. Primary pulmonary IVLBCL should be considered in patients presenting with recurrent fever, GGO in the lungs, and ineffective responses to anti-inflammatory and anti-infection treatments. Timely puncture cytology of the lesion site should be performed to identify the cause of the disease, ensuring that the patients receive accurate treatment effectively. This approach can help avoid misdiagnosis due to nonspecific clinical symptoms.

Acknowledgements

Not applicable.

Funding

No funding was received.

Availability of data and materials

The data generated in the present study may be requested from the corresponding author.

Authors' contributions

WJ and XX were responsible for data analysis and manuscript drafting. ML and CZ were responsible for collecting the data and drafting the work. WJ and XX contributed to design and revised the manuscript critically for important intellectual content. The authors have accepted responsibility for the entire content of this manuscript and approved its submission. WJ and XX confirm the authenticity of all the raw data. All authors have read and approved the final manuscript.

Ethics approval and consent to participate

Not applicable.

Patient consent for publication

The patient provided written informed consent for the publication of this case report.

Competing interests

The authors declare that they have no competing interests.

References

1. Ponzoni M, Campo E and Nakamura S: Intravascular large B-cell lymphoma: A chameleon with multiple faces and many masks. Blood 132: 1561-1567, 2018.
2. Lymphoid Disease Group, Chinese Society of Hematology, Chinese Medical Association; Lymphoma Expert Committee of Chinese Society of Clinical Oncology(CSCO): Chinese expert consensus on the diagnosis and management of intravascular large B cell lymphoma (2023). Zhonghua Xue Ye Xue Za Zhi 44: 177-181, 2023 (In Chinese).

3. Baptista P, Aguiar E, Fonseca E, Pinto R and Trigo F: Intravascular large B-cell lymphoma presenting with haemophagocytic syndrome. Br J Haematol 204: 2151-2152, 2024.
4. Ferreri AJM, Campo E, Seymour JF, Willemze R, Ilariucci F, Ambrosetti A, Zucca E, Rossi G, López-Guillermo A, Pavlovsky MA, *et al*: Intravascular lymphoma: Clinical presentation, natural history, management and prognostic factors in a series of 38 cases, with special emphasis on the 'cutaneous variant'. Br J Haematol 127: 173-183, 2004.
5. Liu Z, Zhang Y, Zhu Y and Zhang W: Prognosis of intravascular large B cell lymphoma (IVLBCL): Analysis of 182 patients from global case series. Cancer Manag Res 12: 10531-10540, 2020.
6. Swerdlow SH, Campo E, Pileri SA, Harris NL, Stein H, Siebert R, Advani R, Ghielmini M, Salles GA, Zelenetz AD and Jaffe ES: The 2016 revision of the World Health Organization classification of lymphoid neoplasms. Blood 127: 2375-2390, 2016.
7. Matsue K, Abe Y, Narita K, Kobayashi H, Kitadate A, Takeuchi M, Miura D and Takeuchi K: Diagnosis of intravascular large B cell lymphoma: Novel insights into clinicopathological features from 42 patients at a single institution over 20 years. Br J Haematol 187: 328-336, 2019.
8. Cakir E, Demirag F and Aydin M: Cytopathologic differential diagnosis of small cell carcinoma and poorly differentiated non-small cell carcinoma in bronchial lavage specimens using a regression analysis. APMIS 118: 150-155, 2010.
9. Ganti AKP, Loo BW, Bassetti M, Blakely C, Chiang A, D'Amico TA, D'Avella C, Dowlati A, Downey RJ, Edelman M, *et al*: Small cell lung cancer, version 2.2022, NCCN clinical practice guidelines in oncology. J Natl Compr Canc Netw 19: 1441-1464, 2021.
10. Debliquis A, Voirin J, Harzallah I, Maurer M, Lerintiu F, Drénou B and Ahle G: Cytomorphology and flow cytometry of brain biopsy rinse fluid enables faster and multidisciplinary diagnosis of large B-cell lymphoma of the central nervous system. Cytometry B Clin Cytom 94: 182-188, 2018.
11. Pinkus GS, Etheridge CL and O'Connor EM: Are keratin proteins a better tumor marker than epithelial membrane antigen? A comparative immunohistochemical study of various paraffin-embedded neoplasms using monoclonal and polyclonal antibodies. Am J Clin Pathol 85: 269-277, 1986.
12. Armitage JO: Staging non-Hodgkin lymphoma. CA Cancer J Clin 55: 368-376, 2005.
13. Murase T, Nakamura S, Kawauchi K, Matsuzaki H, Sakai C, Inaba T, Nasu K, Tashiro K, Suchi T and Saito H: An Asian variant of intravascular large B-cell lymphoma: Clinical, pathological and cytogenetic approaches to diffuse large B-cell lymphoma associated with haemophagocytic syndrome. Br J Haematol 111: 826-834, 2000.
14. Bae HJ, Chon GR, Kim DJ, Lee SH and Ahn JY: A case of intravascular large B-cell lymphoma of lung presenting with progressive multiple nodules on chest computed tomography. Respir Med Case Rep 21: 108-112, 2017.
15. Zhu M, Chang Y, Fan H, Shi J, Zhu B and Mai X: Primary pulmonary intravascular large B-cell lymphoma misdiagnosed as pneumonia: Four case reports and a literature review. Oncol Lett 25: 234, 2023.
16. Nguyen TT, Sekiguchi H, Yi ES and Ryu JH: Occult diffuse neoplasm in the lungs: Intravascular large B-cell lymphoma. Am J Med 134: 926-929, 2021.
17. Davis JW, Auerbach A, Crothers BA, Lewin E, Lynch DT, Teschan NJ and Schmieg JJ: Intravascular large B-cell lymphoma. Arch Pathol Lab Med 146: 1160-1167, 2022.
18. Yamamoto R, Okagaki N, Sakamoto H, Tanaka Y, Takeda A, Maruguchi N, Nakamura S, Matsumura K, Ueyama M, Ikegami N, *et al*: Intravascular large B-cell lymphoma presenting as pulmonary ground-glass nodules that progressed slowly over several months with no overt symptoms. Intern Med 63: 559-563, 2024.
19. Cheng JW and Li JH: Intravascular large B-cell lymphoma. N Engl J Med 389: 2188, 2023.
20. Yu H, Chen G, Zhang R and Jin X: Primary intravascular large B-cell lymphoma of lung: A report of one case and review. Diagn Pathol 7: 70, 2012.
21. Enzan N, Kitadate A, Tanaka A and Matsue K: Incisional random skin biopsy, not punch biopsy, is an appropriate method for diagnosis of intravascular large B-cell lymphoma: A clinicopathological study of 25 patients. Br J Dermatol 181: 200-201, 2019.
22. Matsue K, Abe Y, Kitadate A, Miura D, Narita K, Kobayashi H, Takeuchi M, Enzan N, Tanaka A and Takeuchi K: Sensitivity and specificity of incisional random skin biopsy for diagnosis of intravascular large B-cell lymphoma. Blood 133: 1257-1259, 2019.
23. MacGillivary ML and Purdy KS: Recommendations for an approach to random skin biopsy in the diagnosis of intravascular B-cell lymphoma. J Cutan Med Surg 27: 44-50, 2023.
24. Kim SR, Ko CJ, Nelson CA, Ramachandran S and Gehlhausen JR: Random skin biopsies for diagnosis of intravascular large B-cell lymphoma: Retrospective analysis of 31 biopsies from a US dermatology inpatient consultative service with literature review. J Am Acad Dermatol 88: 714-716, 2023.
25. Rozenbaum D, Tung J, Xue Y, Hoang MP and Kroshinsky D: Skin biopsy in the diagnosis of intravascular lymphoma: A retrospective diagnostic accuracy study. J Am Acad Dermatol 85: 665-670, 2021.
26. Wu F, Wang Z, Xing X, Yu M and Shi B: The Value of 18F-FDG PET/CT in diagnostic procedure of intravascular large B-cell lymphoma presenting fever of unknown origin and pulmonary hypertension as an initial manifestation. Clin Nucl Med 41: 506-507, 2016.
27. Spencer J, Dusing R, Yap W, Hill J and Walter C: Intravascular large B-cell lymphoma presenting with diffusely increased pulmonary fluorodeoxyglucose uptake without corresponding CT abnormality. Radiol Case Rep 14: 260-264, 2018.
28. Mondoni M, Rinaldo RF, Carlucci P, Terraneo S, Saderi L, Centanni S and Sotgiu G: Bronchoscopic sampling techniques in the era of technological bronchoscopy. Pulmonology 28: 461-471, 2022.
29. Thomas RK, Re D, Wolf J and Diehl V: Part I: Hodgkin's lymphoma-molecular biology of Hodgkin and Reed-Sternberg cells. Lancet Oncol 5: 11-18, 2004.
30. Luzuriaga K and Sullivan JL: Infectious mononucleosis. N Engl J Med 362: 1993-2000, 2010.
31. Tanaka Y, Kobayashi Y, Maeshima AM, Oh SY, Nomoto J, Fukuhara S, Kitahara H, Munakata W, Suzuki T, Maruyama D and Tobinai K: Intravascular large B-cell lymphoma secondary to lymphoplasmacytic lymphoma: A case report and review of literature with clonality analysis. Int J Clin Exp Pathol 8: 3339-3343, 2015.
32. Gonzalez-Farre B, Ramis-Zaldivar JE, Castrejón de Anta N, Rivas-Delgado A, Nadeu F, Salmeron-Villalobos J, Enjuanes A, Karube K, Balagué O, Cobo F, *et al*: Intravascular large B-cell lymphoma genomic profile is characterized by alterations in genes regulating NF-κB and immune checkpoints. Am J Surg Pathol 47: 202-211, 2023.
33. Shimada K, Yoshida K, Suzuki Y, Iriyama C, Inoue Y, Sanada M, Kataoka K, Yuge M, Takagi Y, Kusumoto S, *et al*: Frequent genetic alterations in immune checkpoint-related genes in intravascular large B-cell lymphoma. Blood 137: 1491-1502, 2021.
34. Fujikura K, Yamashita D, Yoshida M, Ishikawa T, Itoh T and Imai Y: Cytogenetic complexity and heterogeneity in intravascular lymphoma. J Clin Pathol 74: 244-250, 2021.
35. Breakell T, Waibel H, Schliep S, Ferstl B, Erdmann M, Berking C and Heppt MV: Intravascular large B-cell lymphoma: A review with a focus on the prognostic value of skin involvement. Curr Oncol 29: 2909-2919, 2022.
36. Shimada K, Murase T, Matsue K, Okamoto M, Ichikawa N, Tsukamoto N, Niitsu N, Miwa H, Asaoku H, Kosugi H, *et al*: Central nervous system involvement in intravascular large B-cell lymphoma: A retrospective analysis of 109 patients. Cancer Sci 101: 1480-1486, 2010.
37. Zhang Y, Jia C, Wang W, Zhang L, Cao X, Li J, Zhang W and Zhou D: The interim analysis from a prospective single-center phase 2 study of Zanubrutinib plus R-CHOP in treat-naïve intravascular large B cell lymphoma. Blood 138 (Suppl 1): S3563, 2021.
38. Kato K, Mori T, Kim SW, Sawa M, Sakai T, Hashimoto H, Taguchi J, Oyake T, Kurahashi S, Imada K, *et al*: Outcome of patients receiving consolidative autologous peripheral blood stem cell transplantation in the frontline treatment of intravascular large B-cell lymphoma: Adult lymphoma working group of the Japan society for hematopoietic cell transplantation. Bone Marrow Transplant 54: 1515-1517, 2019.